Society of Petroleum Engineers

SPE-182714-MS

General Implicit Coupling Framework for Multi-Physics Problems

Ruslan Rin, Pavel Tomin, and Timur Garipov, Stanford University; Denis Voskov, TU Delft; Hamdi Tchelepi, Stanford University

This paper was prepared for presentation at the SPE Reservoir Simulation Conference held in Montgomery, TX, USA, 20–22 February 2017.

Abstract

We present a new framework for solving coupled multi-physics problems. The objective is to develop a platform where different coupling strategies for the simulation of complex physical processes can be employed with great flexibility in order to find an optimal - in terms of robustness and computational efficiency - strategy for a given problem. The new simulator is modular; each module represents a particular physics process, such as compositional, thermal, poromechanics, reactions, wells, and surface facilities. The platform provides seamless coupling between the physics modules without resorting to conditional branches and intermediate interface and treats terms that are coupled across multiple physics modules efficiently. The different modules can be coupled with each other in a sequential or fully coupled manner, and different solution strategies can be applied to different modules. This allows investigation of complex coupling strategies that have not been studied before. Examples of target problems include modeling compositional-thermal EOR processes in both conventional and unconventional resources with tight coupling to nonlinear poromechanics. The paper addresses the design of the framework and provides details of its implementation.

Introduction

Simulation of complex subsurface processes entails solution of multiphase flow, multi-component transport of mass and heat. In addition, reactions and mechanical interactions with the solid have received significant attention, especially for the management of unconventional resources. Having a reservoir simulation framework that is easily extensible to account for the additional physical interactions and ‘new’ transport mechanisms associated with Enhanced Oil Recovery (EOR) processes is quite important. To meet this objective, we have to deal with the important challenge of balancing the complexity of the flow physics with computational efficiency. Specifically, it is important to deal with the coupling across the different physical mechanisms while developing specialized discretization and solution schemes for the sub-problems.

In the reservoir engineering community, it is common to employ different simulators for the flow and geomechanics problems; the coupling between the flow and mechanics codes has been the subject of intense activity in the last decade. The coupling schemes can be split across three broad categories (Settari and Walters, 2001), namely, decoupled, iteratively coupled, and fully coupled. While the fully coupled approach, Fully Implicit Method (FIM), ensures unconditionally stable numerical solutions for well-posed problems, it is computationally expensive and requires the development of complex simulation codes

(Hu et al., 2013). Moreover, an appropriate solution technique for the algebraic system resulting from a linearization of the multi-physics (flow, transport, mechanics) problem poses serious scalability issues (White and Borja, 2011; White et al., 2016; Castelletto et al., 2015; Klevtsov et al., 2016). Iterative sequential (SEQ) solution strategies can be effective if the sub-problems (e.g., flow and mechanics) can be solved in a scalable manner. The iterative-implicit approach allows for using specialized linear and nonlinear solvers for each of the sub-problems. If such a sequential-implicit strategy can be used, then the requirements on the linear solver capabilities can be less severe. Unfortunately, depending on the coupling strength across the physical processes (transport, flow, reactions, mechanics), iterative implicit solution strategies may entail slow convergence rates and very large numbers of global (overall) iterations.

When iteratively-coupled and FIM strategies lead to comparable results within the desired tolerance, it is not always clear which strategy would result in the optimal approach, in terms of robustness and computational efficiency, for a given class of problem. In some cases, treatment of a particular part of the coupled problem in a sequential manner may improve convergence (Maes et al., 2016). At the same time, the high complexity of multi-physics simulators prevents from a consistent comparison of different solution strategies. Several authors investigated convergence and performance of different coupling strategies for compositional-thermal-mechanical problems (Alpak, 2015; Bao et al., 2013; Garipov et al., 2016; Kim, 2015). However, to the best of our knowledge, applied strategies were limited to compositional-thermal and mechanical splitting.

We present a new general sequential-implicit coupling framework for solving multi-physics problems related to reservoir simulation. The framework allows for different coupling strategies with great flexibility in order to arrive at robust and scalable solutions for a given class of problem. We demonstrate how different coupling strategies can be accommodated and tested efficiently in our framework. This development represents the next-generation of the Automatic-Differentiation General Purpose Research Simulator (AD-GPRS) (Voskov and Tchelepi, 2012; Zhou, 2012). The new developments preserve all the advanced physical modeling and numerical capabilities in the existing AD-GPRS. The capabilities include the thermal-compositional, EOS-based, multiphase flow and transport models (Zaydullin et al., 2014; Voskov et al., 2016), generalized nonlinear formulations (Voskov, 2012; Zaydullin et al., 2013), multi-stage linear solvers (Zhou et al., 2013; Klevtsov et al., 2016), complex multi-segment wells (Zhou, 2012), and nonlinear mechanical deformation models (Garipov et al., 2015, 2016).

The paper is organized as follows. First, we summarize governing equations and the different coupling strategies. Then, we describe the new general sequential-implicit simulation framework. Then, we validate the new AD-GPRS framework using several problems.

Mathematical Formulation

The proposed framework is applicable for an arbitrary number of physics modules, we limit the description here to thermal multi-component flow in deformable subsurface formations. The full set of governing equations that describes these processes include the conservation of mass, energy, and momentum with constraints and constitutive relations.

Multi-component transport

The mass balance equations for n_c components that can exist in n_p fluid phases can be written as:

$$R_F \equiv \frac{\partial}{\partial t}\left(\phi \sum_{j=1}^{n_p} x_{ij}\rho_j S_j\right) + \nabla \cdot \left(\sum_{j=1}^{n_p} x_{ij}\rho_j \boldsymbol{v}_j\right) + \sum_{j=1}^{n_p} x_{ij}\rho_j q_j = 0, \quad i = 1..n_c, \tag{1}$$

where i is the index of a component, j the index of a phase, ϕ the porosity, x_{ij} the phase compositions, ρ_j the phase density, S_j the phase saturation, q_j the source term. Phase velocity, $\boldsymbol{v}_j$, is given by the Darcy's law

$$\boldsymbol{v}_j = -\frac{\boldsymbol{k}k_{rj}}{\mu_j}\nabla p_j, \tag{2}$$

where $\boldsymbol{k}$ is the absolute permeability, k_{rj} the relative permeability of the phase, μ_j the viscosity of the phase, p_j the phase pressure.

These equations are supplemented with linear constrains for the phase compositions and the phase saturations:

$$\sum_{i=1}^{n_c} x_{ij} = 1,\ \forall j = 1..n_p, \tag{3}$$

$$\sum_{j=1}^{n_p} S_j = 1, \tag{4}$$

and the equality condition for fugacities (instantaneous thermodynamic phase equilibrium is assumed):

$$f_{ij}\left(p,T,x_{ij}\right) - f_{ik}\left(p,T,x_{ik}\right) = 0,\ \forall j \neq k = 1..n_p, i = 1..n_c. \tag{5}$$

Here, we employed the natural-variables formulation (Coats, 1980; Voskov and Tchelepi, 2012), where the primary unknowns are the pressure, p, phase saturations S_j, and phase compositions, x_{ij}.

Conservation of Energy

We assume thermal equilibrium between the rock and the fluids. It follows that the total-energy balance equation can be expressed as:

$$R_T \equiv \frac{\partial}{\partial t}\left(\phi\sum_{j=1}^{n_p} u_j\rho_j S_j + (1-\phi)\,u_r\right) + \nabla\cdot\left(\sum_{j=1}^{n_p} h_j\rho_j\boldsymbol{v}_j\right) - \nabla\cdot(\kappa\nabla T) + \sum_{j=1}^{n_p} h_j\rho_j q_j = 0, \tag{6}$$

where κ is the thermal-conductivity coefficient, u_j the phase internal energies, u_r the rock internal-energy, and h_j the phase enthalpy. The primary unknown related to the energy equations is temperature, T. All the thermal properties are evaluated based on p, T, and x_{ij} using correlations and the particular cubic Equation of State (EoS). The details of the thermal-compositional implementation are given elsewhere (Zaydullin et al., 2014).

Mechanics

The mechanical deformation equations are formulated in terms of total stresses, bulk strains, pore pressure, and temperatures, and then can be written as:

$$R_M \equiv \nabla\cdot\boldsymbol{\sigma} + \rho\boldsymbol{g} = 0, \tag{7}$$

where $\rho = \rho_s(1-\phi) + \rho_f\phi$ is the overall-mass density, ρ_s is the density of solid skeleton and ρ_f is the average fluid density. The total-stress tensor, $\boldsymbol{\sigma}$, contains the contributions of the fluid and solid-skeleton (Coussy, 2004):

$$\boldsymbol{\sigma} = \mathbb{C}\boldsymbol{\varepsilon} - \mathbf{b}\bar{p} - \mathbf{a}T, \tag{8}$$

where $\boldsymbol{\varepsilon} = \frac{1}{2}\left(\nabla\boldsymbol{u} + \nabla^T\boldsymbol{u}\right)$ is the elastic strain tensor, and vector $\boldsymbol{u}$ represents the displacements (primary unknowns). Pressure value, $\bar{p}$, is defined as the average fluid pressure, $\bar{p} = \sum_{j=1}^{n_p} S_j p_j$. We also define the elastic moduli tensor, $\mathbb{C}$, the tensor of Biot's coefficients $\mathbf{b} = b\mathbf{1}$, and the thermal expansion tensor $\mathbf{a} = \alpha\mathbb{C}\mathbf{1}$. Here α is the skeleton linear thermal expansion coefficient, b is the Biot's coefficient, and symbol

1 represents the unit tensor. Further, we accept the next relationship for the porosity calculation (Coussy, 2004):

$$\phi = \phi_0 + \frac{(b-\phi_0)(1-b)}{K_d}(p-p_0) + b(\boldsymbol{\varepsilon}_v - \boldsymbol{\varepsilon}_{v,0}) - \alpha_\phi (T-T_0), \tag{9}$$

where K_d is the local drainage bulk modulus, α_ϕ is the volumetric thermal-dilation coefficient related to the porosity, and ϕ_0, p_0, T_0, and $\boldsymbol{\varepsilon}_{v,0}$ are the reference porosity, pressure, temperature, and volumetric strain, respectively. For permeability calculation we use the following empirical relationship (David et al., 1994):

$$k = k_0 \left(\frac{\phi}{\phi_0}\right)^m, \tag{10}$$

where the exponent, m, defines the change from the reference value k_0. The details of the geomechanical implementation can be found in Garipov et al. (2015).

Coupling Strategies

We define the set of given physics as $\wp$. Next, we introduce the following notation to describe a chosen coupling strategy Ψ:

$$\Psi = \Upsilon_A [A_1, A_2, ..., A_n], \tag{11}$$

where $\Upsilon_A \in \{\text{FIM, SEQ}\}$, and A_i either represents one of the physics ($A; \in \wp$) or refers to another coupled set ($A, = \Upsilon_B [B_1, \ldots, B_k]$, where B_j is defined similarly to A_i). Notice that Υ = FIM is invariant over order of arguments, which is not true for Υ = SEQ.

Here, we assume $\wp$ = {FLOW, THERMAL, MECHANICS}, where FLOW, THERMAL, MECHANICS represent multi-component flow (Eqs. 1-5), thermal (Eq. 6), and mechanics (Eqs. 7-10), respectively. For the given $\wp$ we introduce a vector of unknowns, $x = (x_F, x_T, x_M)$, where x_F are the flow unknowns, x_T the thermal unknowns, and x_M the mechanical unknowns. The corresponding residuals are $R_F(x_F, x_T, x_M)$, $R_T(x_F, x_T, x_M)$, and $R_M(x_F, x_T, x_M)$. For coupled flow, thermal, and mechanics, several coupling strategies can be used. The two mostly used options are briefly outlined below.

Option 1: Fully implicit coupling: solving all the residuals equations simultaneously (Fig. 1):

$$\begin{cases} R_F^{n+1}\left(x_F^{n+1}, x_T^{n+1}, x_M^{n+1}, x^n\right) = 0, \\ R_T^{n+1}\left(x_F^{n+1}, x_T^{n+1}, x_M^{n+1}, x^n\right) = 0, \\ R_M^{n+1}\left(x_F^{n+1}, x_T^{n+1}, x_M^{n+1}, x^n\right) = 0. \end{cases} \tag{12}$$

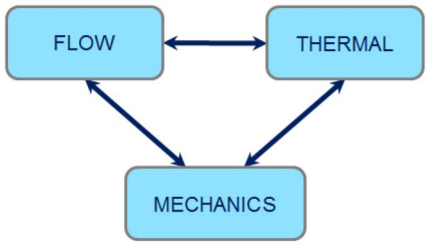

Figure 1—Fully implicit coupling: Ψ=FIM[FLOW, THERMAL, MECHANICS].

Using Newton's method leads to the following system:

$$\begin{bmatrix} \partial R_F/\partial x_F & \partial R_F/\partial x_T & \partial R_F/\partial x_M \\ \partial R_T/\partial x_F & \partial R_T/\partial x_T & \partial R_T/\partial x_M \\ \partial R_M/\partial x_F & \partial R_M/\partial x_T & \partial R_M/\partial x_M \end{bmatrix} \begin{bmatrix} \delta x_F \\ \delta x_T \\ \delta x_M \end{bmatrix} = - \begin{bmatrix} R_F \\ R_T \\ R_M \end{bmatrix}. \tag{13}$$

Option 2: Fully coupled flow and energy-balance, followed by sequentially coupled mechanics (Fig. 2):

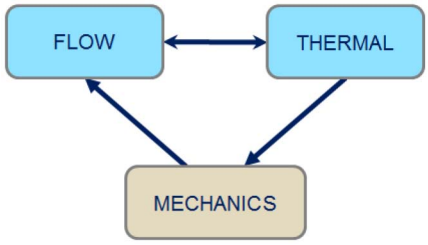

Figure 2—Fully coupled flow and energy-balance, followed by sequentially coupled mechanics: Ψ = SEQ[FIM(FLOW, THERMAL), MECHANICS].

Step 1: Solve

$$\begin{cases} R_F^{n+1}\left(x_F^{n+1}, x_T^{n+1}, x_M^{n+1/2}, x^n\right) = 0, \\ R_T^{n+1}\left(x_F^{n+1}, x_T^{n+1}, x_M^{n+1/2}, x^n\right) = 0. \end{cases} \tag{14}$$

or in the linearized matrix form

$$\begin{bmatrix} \partial R_F/\partial x_F & \partial R_F/\partial x_T \\ \partial R_T/\partial x_F & \partial R_T/\partial x_T \end{bmatrix} \begin{bmatrix} \delta x_F \\ \delta x_T \end{bmatrix} = - \begin{bmatrix} R_F \\ R_T \end{bmatrix}. \tag{15}$$

Step 2: Solve

$$R_M^{n+1}(x_F^{n+1}, x_T^{n+1}, x_M^{n+1}, x^n) = 0. \tag{16}$$

matrix form

$$\left[\partial R_M/\partial x_M\right]\left[\delta x_M\right] = -\left[R_M\right]. \tag{17}$$

There are 13 different coupling strategies for problems involving multiphase flow, thermal effects, and mechanical deformation.

FIM[FLOW, THERMAL, MECHANICS]		
SEQ[FIM(FLOW, THERMAL), MECHANICS]	SEQ[FLOW, FIM(THERMAL, MECHANICS]	SEQ[MECHANICS, FIM(FLOW, THERMAL)]
SEQ[FIM(MECHANICS, FLOW), THERMAL]	SEQ[THERMAL, FIM(FLOW, MECHANICS)]	SEQ[FIM(THERMAL, MECHANICS), FLOW]
SEQ[FLOW, THERMAL, MECHANICS]	SEQ[FLOW, MECHCANICS, THERMAL]	SEQ[THERMAL, FLOW, MECHANICS]
SEQ[THERMAL, MECHANICS, FLOW]	SEQ[MECHANICS, FLOW, THERMAL]	SEQ[MECHANICS, THERMAL, FLOW]

For problems with four physics modules (e.g., flow, thermal, mechanics, reactions), the number of coupling strategies is 49. This would require implementing a large number of different simulators, which is simply not doable. Although not all coupling strategies are potentially useful, numerical analysis of these

solution schemes is often limited to simplified physics (Kim et al., 2013; Kim, 2015). In modeling coupled nonlinear dynamics problems, it is often the case that one has to experiment with different schemes to figure out what works best for which problem class. Our focus here is a tool that allows for implementing, testing, and comparing different coupling strategies in a unified simulation framework with advanced reservoir flow simulation capabilities.

Framework Design

We employ a modular design by splitting a given multi-physics problem into a set of sub-problems. Each sub-problem represents a particular physics process, e.g., flow, thermal, reactions, mechanics, wells. Each subproblem may have its own computational domain, nonlinear formulation, and spatial discretization. The focus of the framework is to build different physics modules, each with a clearly defined interface. Flexibility in coupling the different sub-problems is of prime importance. The objective is to provide wide flexibility in the number of different physics modules and how they are coupled. The choice of the coupling strategy is part of the simulation input. To allow this level of flexibility, two important questions have to be answered. First: how to solve each sub-problem for a particular coupling strategies? Second: how to stitch all the sub-problems together to produce a global numerical solution for a given timestep. In the following section, we outline the basis of sub-problems organization. Then, we describe the strategy for accommodating complex coupling terms and properties.

Subsets

The concept of subsets lies at the core of the new AD-GPRS. A subset is an abstract computational domain with a defined set of unknowns and properties. For example, the flow physics module may have a cellbased subset with unknowns, such as p, and S_j and properties, such as k_{rj}, μ_j. In addition, we may define a connection-based subset with unknowns defined at the interfaces of a control-volume, e.g. phase velocities $\boldsymbol{v}_j$. The geomechanics module employs vertex-based displacements, $\boldsymbol{u}$, and cell-based properties, such as the averaged fluid pressure $\bar{p}$ volumetric strain $\boldsymbol{\varepsilon}_v$, and volumetric stress $\boldsymbol{\sigma}_v$.

The overall flexibility of the framework depends strongly on how subsets are designed and implemented. For example, subsets of properties defined on a fine grid and also on a coarse grid allow for multiscale formulations and solution schemes, while connection-based subsets allow for decoupling the accumulation and flux parts in the low-order transport equations. Fig. 3 shows an example of physics modules and the decomposition into subsets for a generic multi-physics problem.

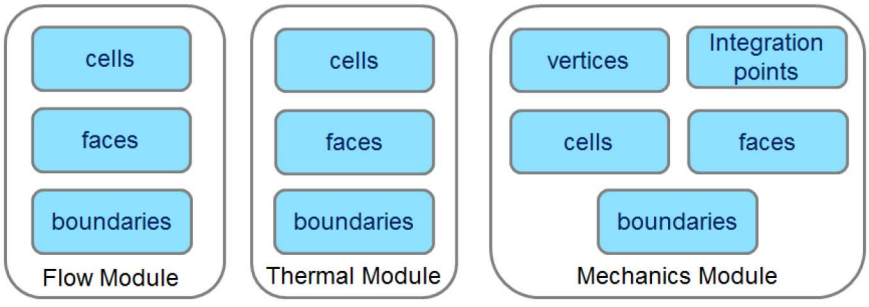

Figure 3—Physics modules (sub-problems) and their hypothetical subsets. Table 1 lists corresponding properties and unknowns for each subset.

Table 1—Example of subsets properties and unknowns.

Sub-problem	Subset	Unknowns and properties
FLOW	cells	$p, S_j, x_{ij}, \mu, \rho, \ldots$
	faces	v^j
	boundaries	boundary conditions
THERMAL	cells	$T, h_j, u_j, h_{tot}, \ldots$
	faces	v_j^e
	boundaries	boundary conditions
MECHANICS	vertices	**u**
	cells	$\bar{p}$
	faces	traction values
	integration points	**ε, σ**, C…
	boundaries	boundary conditions

Sub-Problem Tree Structure and Global Status Table

A tree structure provides a general representation of a given coupling scheme. Each internal node in the tree defines a coupling strategy −ϒ (FIM or SEQ) - that is applied to the children nodes. Each terminal node in the tree represents particular physics problem with a dedicated linear solver. Fig. 4 shows several examples of a tree structure for a particular coupling scheme for a given multi-physics problem.

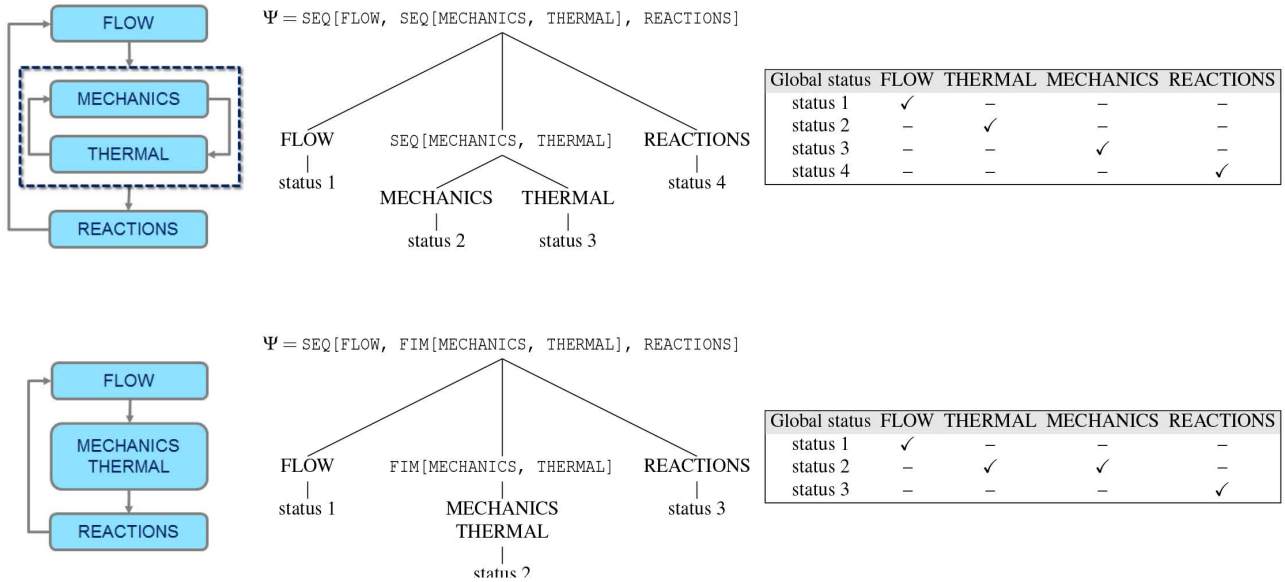

Figure 4—The coupling strategy for the first example (top) is Ψ = SEQ[FLOW, SEQ(MECHANICS, THERMAL), REACTIONS], where the global sequential approach is used to couple all the sub-problems together (Υ_A = SEQ), and the geomechanics and thermal sub-problems are solved sequentially (Υ_B = SEQ). The second example (bottom) also employs the global sequential coupling strategy Ψ = SEQ[FLOW, FIM(MECHANICS, THERMAL), REACTIONS], but the geomechanics and thermal subproblems are solved in a fully implicit manner (Υ_B = FIM). The corresponding global status tables are shown on the right side. Each global status defines which sub-problems and corresponding subsets are activated. For the third example, status 1 activates FLOW, and status 3 activates REACTIONS. Status 2 activates THERMAL and MECHANICS simultaneously. A particular linear solver choice can be associated with a given status.

We define status as a specific choice and ordering of the problem unknowns. The status change may involve dynamic variable switching, which is used in various formulations of multiphase flow models when

phases appear or disappear. Moreover, it is often the case that the number of independent unknowns is different for different situations (e.g., different phase states), which imply that the size of the residual vector and the Jacobian matrix can change.

The Automatically Differentiable Expression Templates Library (ADETL) (Younis, 2011; Zhou, 2012) provides a possibility to define a status table for each subset and automatically rearranges the column structure and enumeration of the variables when the status changes. All possible statuses with independent unknowns are defined as active. The new framework extends the status table concept by adding an auxiliary inactive status without independent unknowns (i.e., all variables are constant) for which derivatives are not formed. Consequently, a subset can be in an active, or inactive, state at any given moment. All possible states form the global status table, which controls the activation and deactivation logic of the subsets. Examples of global status tables for different trees are demonstrated in Fig. 4.

When all the physics-module subsets are active, a full Jacobian matrix is formed, and the fully implicit strategy is applied. However, if one of the physics module is in the inactive state, no derivatives will be constructed for this subset. This approach has several advantages: (1) the desired coupling strategy can be chosen by activating and deactivating specific subsets; (2) facilitates efficient code design: no specific property storage, conditional branches or interfaces are required to couple physics modules that use a sequential strategy; (3) avoids excessive copying of data between physics modules, (4) allows for testing hybrid schemes: we can employ fully coupled strategy for strongly coupled domains of the problem and apply a sequentially coupled strategy for the rest (e.g., see (Tomin and Lunati, 2015)).

Algorithm 1 summaries how a given coupling strategy can be applied based on a tree structure and the global status table.

Algorithm 1—Node solve function pseudocode. The function is called recursively in the sub-problems tree passing algorithm. Here node is the sub-problem tree node, *node.children* gives an ordered set of corresponding children elements.

```
function SOLVE(node)
    if node is terminal then
        Activate global status
        Solve current problem using dedicated linear solver
    else
        n_it = 0
        while n_it < n_it^max do
            n_it = n_it + 1
            for all i ϵ node.children do
                if SOLVE(node.children[i]) is not converged then return fail ▷ stop in case of convergence problem
            end for
            if node globally converged then return success
        end while
end function
```

Coupling Properties

Another important question to be addressed is how to treat coupling properties that are shared by several physics modules. For example, porosity ϕ (see Eq. 9) is a function of cell pressure p (flow subset), volumetric strain ε_v, and mean stress σ_v (mechanics subsets), while the phase viscosity μ_j is a function of pressure p, phase saturation S_j, compositions x_{ij} (flow subsets), and temperature T or enthalpy H (thermal subset). Fig. 5 represents an example of a coupled property.

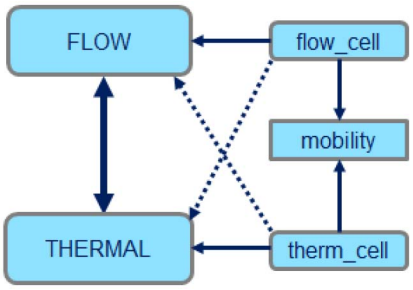

Figure 5—A coupled property example. Here we have two sub-problems FLOW and THERMAL with corresponding flowcell and therm_cell subsets. Solid lines between sub-problems and subsets indicate that properties defined in the subset can be changed, while dashed lines - cannot. Mobility is a coupled property because it depends on pressure and composition from flowcell subset, and on temperature from thermcell subset.

Here, whenever we apply a global status switch, we calculate all 'coupled properties' first, followed by computation of the properties that are associated with sub-problems. This guarantees correctness of derivatives produced by automatic differentiation. Moreover, we can update related coupled properties when the corresponding subset is updated. Thus, a coupled property can be interpreted as a sub-problem without governing equations.

Numerical Examples

Flow-Thermal Coupling: Advonin's Problem

We consider a geothermal problem (Avdonin, 1964; Wong et al., 2015). This test case involves a one-dimensional linear steady-state flow and unsteady heat transport of single-phase liquid water. Cold water at T = 423 K is injected with a flow rate of $q = 10\ \mathrm{m}^3$/day into a reservoir with water at T = 473 K. The boundary condition imposed is a pressure of $50 \cdot 10^5$ Pa at an outer radius of 1000 m. The model properties are shown in Table 2. Fig. 6 shows the temperature distribution at t = 1000 days and the temperature evolution at x = 25 m, both using FIM

$$\Psi_1 = \texttt{FIM[FLOW, THERMAL]}, \tag{18}$$

and SEQ

$$\Psi_2 = \texttt{SEQ[FLOW, THERMAL]}. \tag{19}$$

Table 2—Parameters for Advonin's problem.

Reservoir length, m	1000
Reservoir thickness, m	100
Rock permeability, mD	1000
Rock density, kg/m^3	2500
Rock specific heat capacity, J/(g-K)	1.0
Porosity	0.2
Spatial grid	uniform 10 m grid spacing

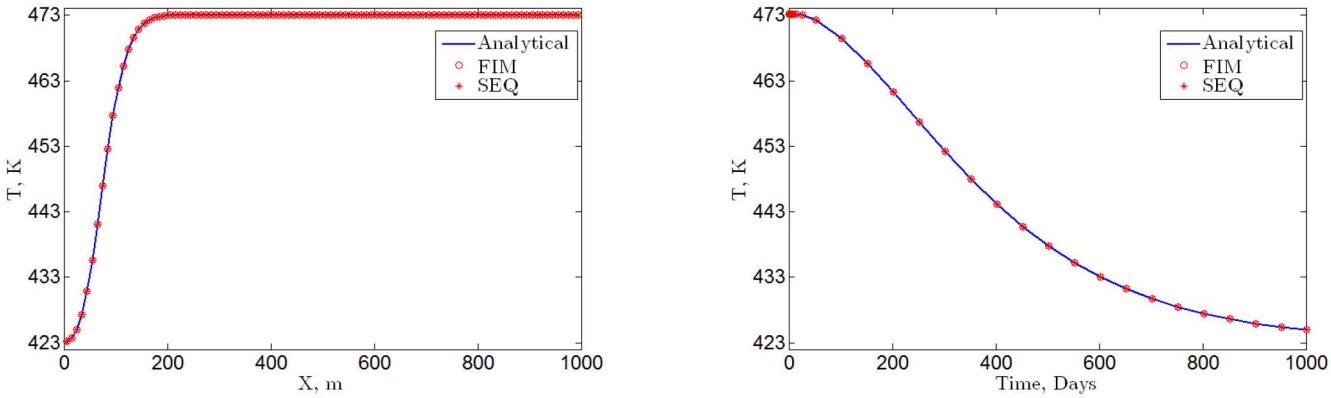

Figure 6—Comparison of the analytical and numerical solutions for the temperature distribution for Advonin problem at t = 1000 days (left), and the temperature evolution at location x = 25 (right).

The sequential approach normally requires 3-7 iterations with tolerance $\varepsilon = 10^{-6}$ to accurately capture the analytical solution (Fig. 7).

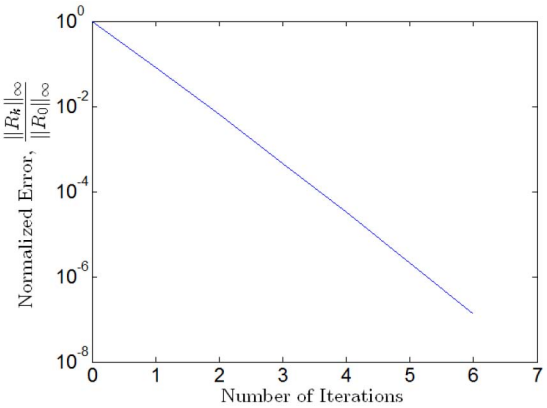

Figure 7—Sequentially implicit method convergence profile after first time step Δt = 0.001 days.

Flow-Mechanical Coupling: Mandel Problem

We consider a two-dimensional Mandel consolidation problem (Mandel, 1953). This example shows the applicability of the presented framework to solve a coupled flowmechanics problems. The problem setup is sketched on Fig. 8. The computational domain $\Omega = [0, a] \times [0, b] = [0{,}20\text{ m}] \times [0{,}10\text{ m}]$ is fully saturated with a slightly compressible single-phase fluid. All domain boundaries are impermeable, except for the right boundary where a constant pressure is enforced, $p|_{x=a} = 0$. The initial fluid pressure is equal to $p|_\Omega = 44.17 \cdot 10^5$Pa. We set zero horizontal displacement on the left boundary ($u_x|_{x=0} = 0$), zero vertical displacement on the bottom boundary ($u_z|_{z=0} = 0$), and uniform loading conditions on the top boundary ($F|_{z=b} = 100 \cdot 10^5$Pa) and $u_z|\forall_{x,\, z=b} = constant$. The model properties are shown in Table 3. We use the undrained Poisson ratio to initialize the displacement field and the drained Poisson ratio to perform the transient simulation. Again, we consider two coupling schemes: FIM

$$\Psi_1 = \texttt{FIM[FLOW, MECHANICS]}, \tag{20}$$

and SEQ

$$\Psi_2 = \texttt{SEQ[FLOW, MECHANICS]}. \tag{21}$$

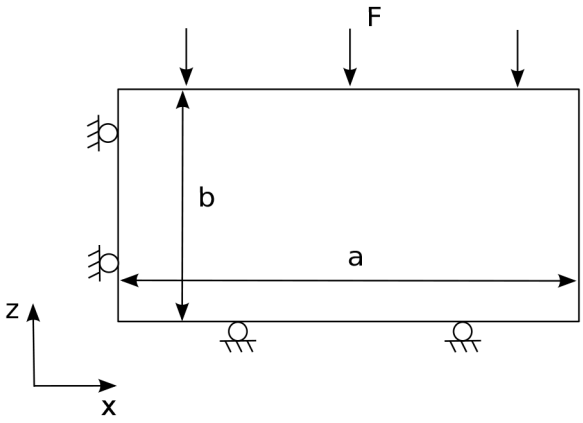

Figure 8—Mandel's problem setup.

Table 3—Rock and fluid properties used for Mandel's problem.

Reference porosity, %	20
Young's modulus, Pa	$1 \cdot 10^{9}$
Biot's constant	1.0
Poisson's ratio	0.25
Undrained Poisson's ratio	0.47
Permeability, mD	1.0
Fluid viscosity, Pa · s	$9.81 \cdot 10^{-5}$
Fluid compressibility, Pa^{-1}	$2 \cdot 10^{-10}$
Reference fluid density, kg/m^3	1000.0

We employ the widely used fixed-stress sequential scheme that guarantees stable convergence behavior (Mikelic and Wheeler, 2013; Kim et al., 2013). Fig. 9 shows the settlement and pressure evolution. Both FIM and SEQ approaches accurately reproduce transient solution behavior, and the sequential approach requires 3-20 iterations with tolerance $\varepsilon = 10^{-6}$ (Fig. 10) which is consistent with the published results (Castelletto et al., 2015).

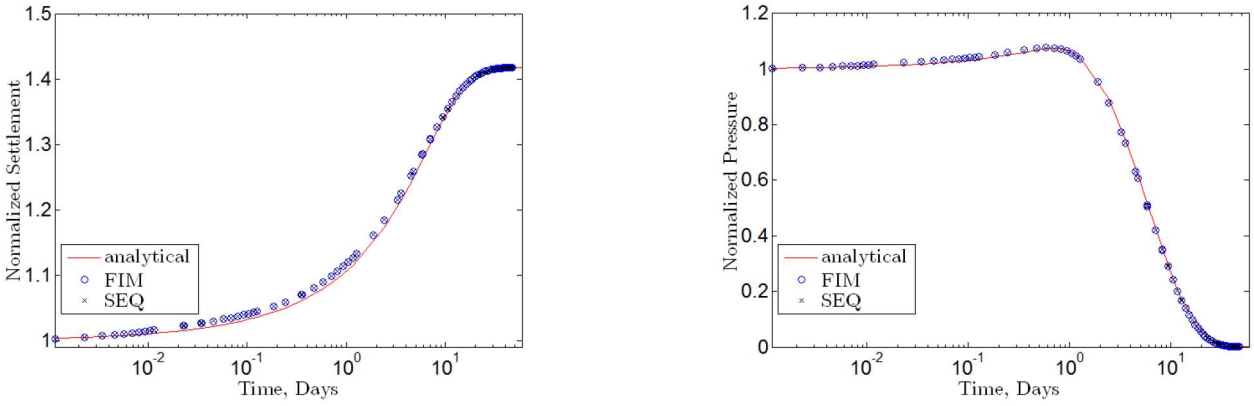

Figure 9—Comparison of the analytical and the numerical solutions for settlement at location (x = 0, z = 100) (left), and pressure at location (x = 2.5, z = 0) (right).

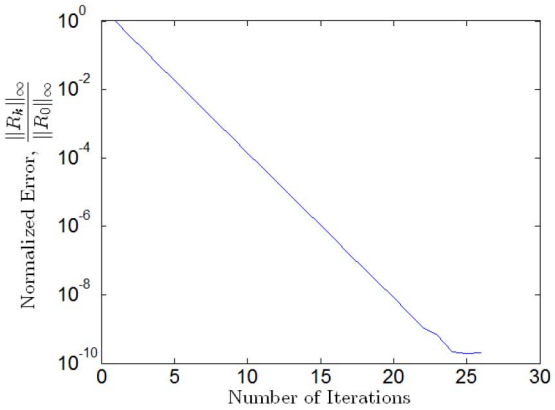

Figure 10—Sequentially implicit method convergence profile for Mandel's problem after first time step Δt = 0.001 days.

Flow-Thermal-Mechanical Coupling: Cold Water Injection Here, we consider a thermal-compositional-mechanical problem. We demonstrate the applicability of the proposed framework to solve problems of practical interest. A modified version of the SPE 9 model (Killough, 1995) is considered (Fig. 11). We extend the description from three-phase black-oil one to a 5-components system (H_2S, C_1, C_5, C_{13}, H_2O). The K-values flash algorithm (Rannou et al., 2013; Zaydullin, 2015) is used for the phase equilibrium calculations. There are 25 producers and 1 injector. All the wells operate with a BHP control. The model parameters are summarized in Table 4.

Table 4—Main parameters for cold water injection problem. See (Killough, 1995) for full specifications of the reservoir properties.

Grid dimensions	24 × 25 × 24
Grid block size in X and Y directions, m	91.44
Reservoir depth range, m	2735.14 − 3231.52
Reservoir dip in X direction, deg	10
Reservoir layers thickness, m	6.1, 4.6, 7.9, 4.6, 4.9, 4.3, 2.4, 2.4, 5.5, 3.7, 5.8, 5.5, 6.1, 15.2, 30.5
Young's modulus, Pa	$2 \cdot 10^9$
Biot's constant	1.0
Poisson's ratio	0.25
Undrained Poisson's ratio	0.47
Rock density, kg/m^3	2250.0
Rock thermal expansion, 1/K	$2 \cdot 10^{-5}$
Rock heat capacity, kJ/(kg K)	2000.0
Rock thermal conductivity, kJ/(m day K)	150.0
Oil thermal conductivity, kJ/(m day K)	11.5
Gas thermal conductivity, kJ/(mdayK)	3.586
Water thermal conductivity, kJ/(m day K)	53.5
Initial reservoir overall composition	0.049, 0.18, 0.6, 0.157, 0.014
Initial reservoir temperature, K	343.0
BHP, Pa	10^7 for producers, $4 \cdot 10^7$ for injector
Injection temperature, K	323.0
Relative phase permeability	$k_{rj} = S_j^2$

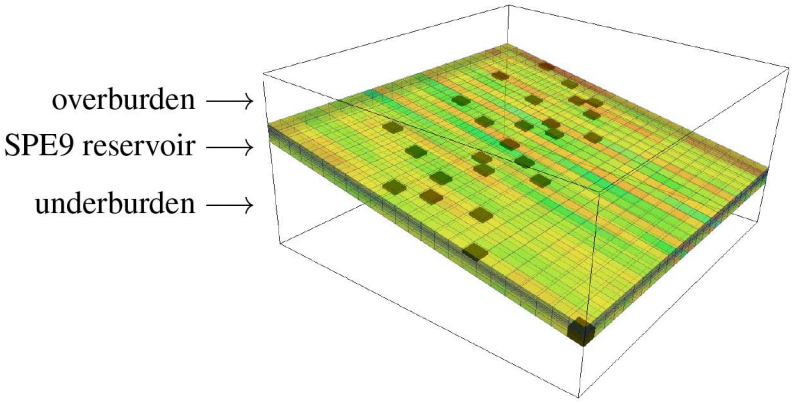

Figure 11—Cold water injection problem. The domain includes the overburden, under-burden, and the reservoir. The reservoir geometry, porosity, permeability, wells locations are from the SPE9 problem. The permeability field is shown and black blocks represent the wells locations.

Here, our starting point and reference is the fully coupled solution obtained using

$$\Psi_1 = \texttt{FIM[FLOW,THERMAL, MECHANICS]}. \tag{22}$$

For the sequential simulations, we again apply the fixed-stress splitting (Kim, 2015). In the first setup, the flow and thermal problems are solved together, followed by the mechanical step:

$$\Psi_2 = \texttt{SEQ[FIM(FLOW, THERMAL), MECHANICS]}. \tag{23}$$

The method requires 3-10 iterations to converge with a tolerance $\varepsilon = 10^{-4}$ (Fig. 12). The SEQ simulation results agree with the FIM solution. Fig. 13 shows the final saturation and temperature distributions together with the differences between FIM and SEQ results. The calculated production and injection rates are also nearly identical (Fig. 14).

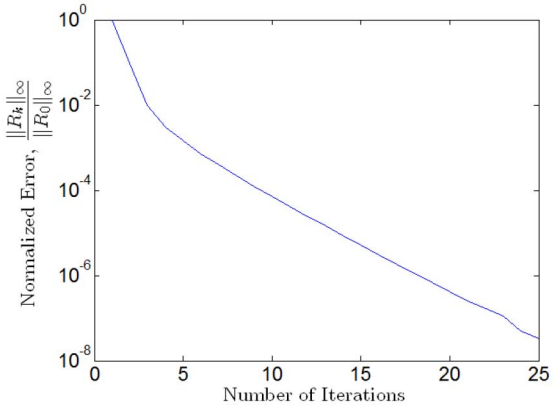

Figure 12—Sequentially implicit method convergence profile for Cold Water Injection problem after first time step Δt = 0.001 days.

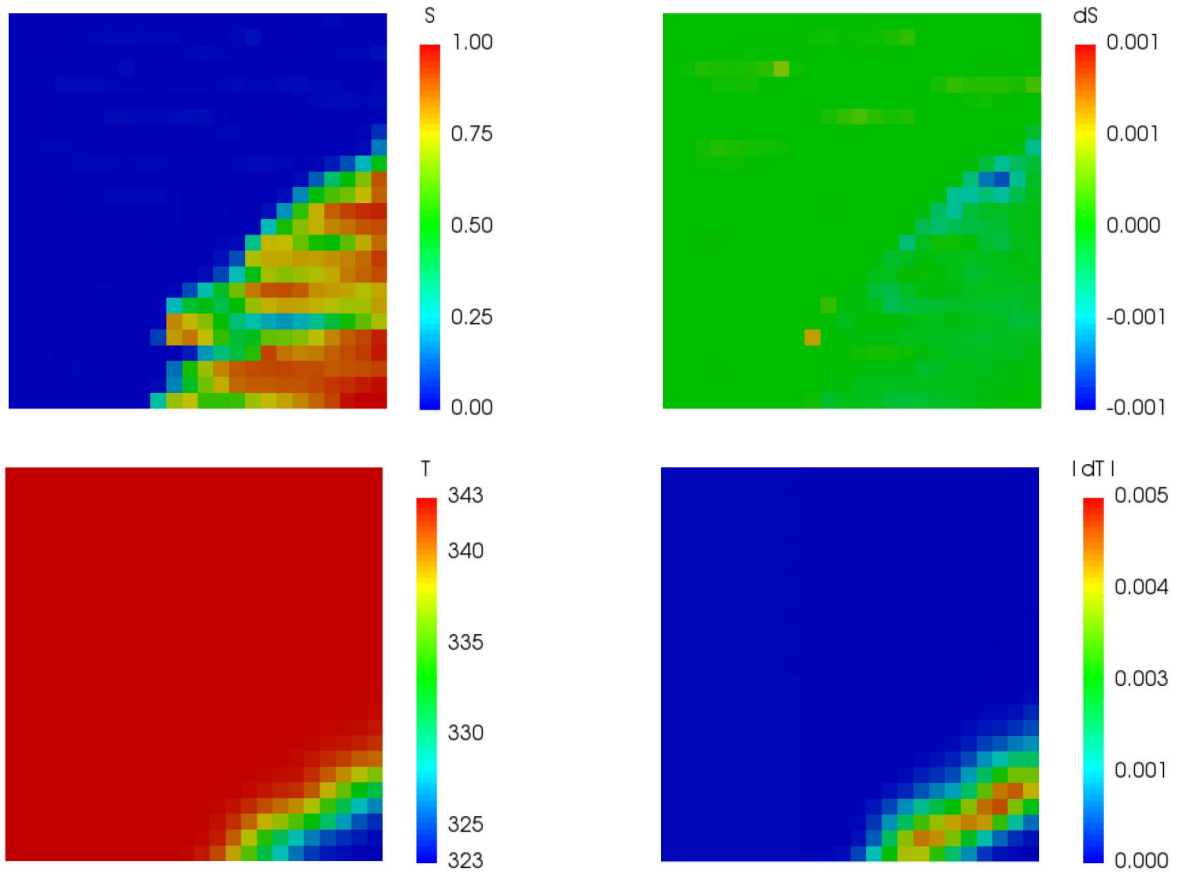

Figure 13—Saturation and temperature distributions in the middle of the reservoir at the end of simulation for FIM approach (left) and difference in them between FIM and SEQ simulations (right).

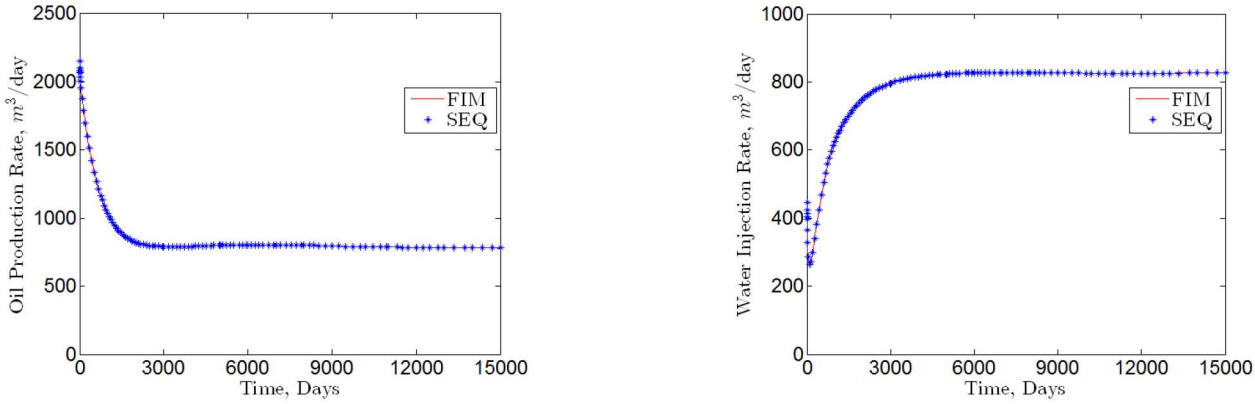

Figure 14—Oil production and water injection rates. FIM and SEQ approaches produce nearly identical results.

Next, we run the sequential algorithm in the nested way: internal sequential loop is between flow and thermal problems and external loop is between flow-thermal block and geomechanics:

$$\Psi_3 = \texttt{SEQ[SEQ(FLOW, THERMAL), MECHANICS]}. \tag{24}$$

The scheme is able to reproduce the fully coupled solution, however, it experiences substantial stability problems and can not converge for the same time steps as the FIM method (the average time step is about two times smaller). The investigation of stable coupling schemes for multiphase thermal problems is a subject of our future research.

Conclusions

We presented a new general implicit coupling framework for solving multi-physics problems, where different coupling strategies can be employed with great flexibility. The objective of this work is to build a powerful and flexible platform to increase the robustness and expand our capabilities in modeling complex multi-physics problems. The new AD-GPRS framework has a modular design where a multi-physics problem is split into a set of sub-problems. Each sub-problem represents a particular physics, e.g., flow, thermal, reactions, mechanics. All of the sub-problems can be solved separately, and then coupled iteratively, or a fully implicit strategy can be used; the new framework also allows for every possible combination in between the purely sequential-implicit and the fully implicit strategies. Thus, the new simulator can be used as an efficient tool to build and compare coupling strategies within the same framework.

We validated the proposed approach using three challenging problems: a problem with flow of mass and energy, a Mandel-type problem for coupling flow and mechanics, and a modified SPE 9 problem with coupled flow of mass, energy, and geomechanics. For each case, we applied at least two different coupling strategies: fully implicit and iterative sequential-implicit coupling. In all cases, both strategies produce similar results.

Acknowledgements

Funding by the Industrial Affiliates Consortium on Reservoir Simulation at Stanford University (SUPRI-B) is appreciated. The authors are grateful to Kirill Terekhov and Yang Wong for valuable discussions and very helpful ideas.

References

Alpak, F. (2015). Robust fully-implicit coupled multiphase-flow and geomechanics simulation. *SPE Journal*, **20** (06).

Avdonin, N. A. (1964). Some formulas for calculating the temperature field of a stratum subject to thermal injection. *Neft'i Gaz*, **3**: 37–41.

Bao, X., Deng, H., Zhong, H., Liu, H., Chen, Z. J., and Dong, C. C. (2013). Coupled geomechanical and thermal simulation of SAGD process. In SPE Heavy Oil Conference-Canada. *Society of Petroleum Engineers*.

Castelletto, N., White, J., and Tchelepi, H. (2015). Accuracy and convergence properties of the fixed-stress iterative solution of two-way coupled poromechanics. *International Journal for Numerical and Analytical Methods in Geomechanics*, **39** (14): 1593–1618.

Coats, K. H. (1980). An equation of state compositional model. *Society of Petroleum Engineers Journal*, **20** (05): 363–376.

Coussy, O. (2004). *Poromechanics*. John Wiley and Sons Ltd.

David, C., Wong, T.-F., Zhu, W., and Zhang, J. (1994). Laboratory measurement of compaction-induced perme ability change in porous rocks: Implications for the generation and maintenance of pore pressure excess in the crust. *Pure and Applied Geophysics*, **143**(1-3):425–456.

Garipov, T., Voskov, D., and Tchelepi, H. A. (2015). Rigorous coupling of geomechanics and thermal-compositional flow for SAGD and ES-SAGD operations. In SPE Canada Heavy Oil Technical Conference. *Society of Petroleum Engineers*.

Garipov, T. T., White, J., Lapene, A., and Tchelepi, H. A. (2016). *Thermo-hydro-mechanical model for source rock thermal maturation*. In 50th US Rock Mechanics/Geomechanics Symposium, Houston, USA. Society of Petroleum Engineers.

Hu, L., Winterfeld, P. H., Fakcharoenphol, P., and Wu, Y.-S. (2013). A novel fully-coupled flow and geomechanics model in enhanced geothermal reservoirs. *Journal of Petroleum Science and Engineering*, **107**: 1–11.

Killough, J. (1995). Ninth SPE comparative solution project: a reexamination of black-oil simulation. In *SPE Reservoir Simulation Symposium*. Society of Petroleum Engineers.

Kim, J. (2015). Unconditionally stable sequential schemes for thermoporomechanics: Undrained-adiabatic and extended fixed-stress splits. In *SPE Reservoir Simulation Symposium*. Society of Petroleum Engineers.

Kim, J., Tchelepi, H. A., and Juanes, R. (2013). Rigorous coupling of geomechanics and multiphase flow with strong capillarity. *SPE journal*, **18** (06): 1–123.

Klevtsov, S., Castelletto, N., White, J. A., and Tchelepi, H. A. (2016). Block-preconditioned Krylov methods for coupled multiphase reservoir flow and geomechanics. In ECMOR XIV-15th European Conference on the Mathematics of Oil Recovery.

Maes, J., Muggeridge, A. H., Jackson, M. D., Quintard, M., and Lapene, A. (2016). Modelling in-situ upgrading of heavy oil using operator splitting method. *Computational Geosciences*, **20** (3): 581–594.

Mandel, J. (1953). Consolidation des sols (etude mathematique). *Geotechnique*, **3** (7): 287–299.

Mikelic, A. and Wheeler, M. (2013). Convergence of iterative coupling for coupled flow and geomechanics. *Computational Geosciences*, **17** (3): 455–461.

Rannou, G., Voskov, D., and Tchelepi, H. A. (2013). Tie-line-based K-value method for compositional simulation. *SPE Journal*, **18** (06): 1–112.

Settari, A. and Walters, D. A. (2001). Advances in coupled geomechanical and reservoir modeling with applications to reservoir compaction. *Spe Journal*, **6** (03): 334–342.

Tomin, P. and Lunati, I. (2015). Local-global splitting for spatiotemporal-adaptive multiscale methods. *Journal of Computational Physics*, **280**: 214–231.

Voskov, D. (2012). An extended natural variable formulation for compositional simulation based on tie-line parameterization. *Transport in Porous Media*, **92** (3): 541–557.

Voskov, D., Zaydullin, R., and Lucia, A. (2016). Heavy oil recovery efficiency using SAGD, SAGD with propane co-injection and STRIP-SAGD. *Computers & Chemical Engineering*, **88**: 115–125.

Voskov, D. V. and Tchelepi, H. A. (2012). Comparison of nonlinear formulations for two-phase multi-component eos based simulation. *Journal of Petroleum Science and Engineering*, **82**: 101–111.

White, J. A. and Borja, R. I. (2011). Block-preconditioned Newton-Krylov solvers for fully coupled flow and geomechanics. *Computational Geosciences*, **15** (4): 647–659.

White, J. A., Castelletto, N., and Tchelepi, H. A. (2016). Block-partitioned solvers for coupled poromechanics: A unified framework. *Computer Methods in Applied Mechanics and Engineering*, **303**: 55–74.

Wong, Z. Y., Horne, R., and Voskov, D. (2015). *A geothermal reservoir simulator in AD-GPRS*. In World Geothermal Congress 2015, Melbourne, Australia. Stanford University.

Younis, R. (2011). *Modern Advances in Software and Solution Algorithms for Reservoir Simulation*. PhD thesis, Stanford University.

Zaydullin, R. (2015). *Compositional space parameterization methods for thermal-compositional simulation*. PhD thesis, Stanford University.

Zaydullin, R., Voskov, D., James, S., Henley, H., and Lucia, A. (2014). Fully compositional and thermal reservoir simulation. *Computers and Chemical Engineering*, **63**: 51–65.

Zaydullin, R., Voskov, D., and Tchelepi, H. (2013). Nonlinear formulation based on an equation-of-state free method for compositional flow simulation. *SPE Journal*, **18** (2): 264–273.

Zhou, Y. (2012). *Parallel general-purpose reservoir simulation with coupled reservoir models and multi-segment wells*. PhD thesis, Stanford University.

Zhou, Y., Jiang, Y., and Tchelepi, H. A. (2013). A scalable multistage linear solver for reservoir models with multisegment wells. *Computational Geosciences*, **17** (2): 197–216.